ELSEVIER

International Journal of Mass Spectrometry 204 (2001) 31–46

International Journal of Mass Spectrometry

Determination of copper binding sites in peptides containing basic residues: a combined experimental and theoretical study

Brian K. Bluhm[1], Sharon J. Shields[2], Craig A. Bayse[3], Michael B. Hall, David H. Russell*

Laboratory for Biological Mass Spectrometry, Department of Chemistry, Texas A&M University, P.O. Box 30012, College Station, TX 77842-3012, USA

Received 7 February 2000, accepted 6 March 2000

Abstract

The energetics of monodentate Cu^+ binding to model systems representing amino acid side chains and bidentate Cu^+ binding in amino acid residues are investigated using electronic structure methods. Results from these calculations are compared with mass spectral data to determine Cu^+ binding sites for gas-phase $[M+Cu]^+$ peptide ions. Calculated monodentate Cu^+ binding energies for amino acid models predict a relative Cu^+ affinity ordering: arg > his > lys > cys > ser, whereas bidentate Cu^+ binding energies give a relative Cu^+ affinity ordering of arg > lys > his > gln > asn > glu> asp. Calculated results are in agreement with current and published experimental results. (Int J Mass Spectrom 204 (2001) 31–46) © 2001 Elsevier Science B.V.

Keywords: MP2 perturbation theory; Post-source decay

1. Introduction

Transition metal ions play important roles in many chemical and biochemical processes (e.g. catalysis and O_2 transport); thus, it is important to develop a detailed understanding of specific binding sites and bond energies for such chemical systems. Although most knowledge concerning transition metal ion chemistry is derived from solution and solid-state studies [1], gas-phase investigations permit us to probe interactions in the absence of solvent, thereby eliminating solvent stabilization of metal ion–ligand interactions [2,3]. In addition, because many biomolecules (e.g. peptides and proteins) contain acidic or basic residues, the charge state of a molecule is dependent on the solvent environment, which can affect complexation of metal ions. Comparison of gas-phase and solution-phase structures yields important information regarding solvent effects on molecular structure. Results from gas-phase data are also readily compared to high level theoretical calculations afforded by recent advances in computers and the availability of quantum chemical software packages [4,5].

* Corresponding author. E-mail: Russell@mail.chem.tamu.edu

[1] Present address: Los Alamos National Laboratory, Nuclear Materials and Technology Division, Actinide Process Chemistry (NMT-2), MS J585, Los Alamos, NM 87545

[2] Present address: Lawrence Livermore National Laboratory, MS L-231, Livermore, CA 94550

[3] Present address: Michigan Technological University, Dept. of Chemistry, 1400 Townsend Drive, Houghton, MI 49931

PII S1387-3806(00)00340-7

Shields and co-workers [6] recently developed a matrix-assisted laser desorption ionization (MALDI) method for producing abundant $[M+Cu]^+$ peptide and protein ions. These studies raise questions concerning Cu^+ binding sites and the effects of binding energies on fragmentation reactions for gas-phase $[M+Cu]^+$ relative to $[M+H]^+$ ions. The prevailing view for $[M+H]^+$ is that the ionizing proton is highly mobile, resulting in charge delocalization with fragmentation occurring at many sites along the peptide backbone [7]. Conversely, alkali metal ions and transition metal ions preferentially bind at specific sites of the molecule and give rise to greater selectivity for bond cleavage [8]. Gas-phase biomolecules complexed with alkali cations have been extensively studied [9–13]; however, there are far fewer studies of transition metal ions complexed to biomolecules [14,15]. Because metal centers may be located in hydrophobic pockets of proteins, gas-phase experiments and ab initio calculations provide more accurate information on intrinsic transition metal ion interactions [16]. Copper, in particular, is interesting due to its involvement with O_2 transport and electron transfer in proteins and enzymes [17].

In earlier articles [6,18] we reported the unimolecular decay chemistry of $[M+Cu]^+$ peptide ions and suggested that Cu^+ binds to basic amino acid side chains, thus liberating a proton to migrate along the peptide chain leading to dissociation, similar to the mobile proton model. This article focuses on our studies of the binding energetics of Cu^+ to peptides containing amino acids with basic side chains, viz. arginine, lysine, and histidine. Previous studies [6,18] suggest that Cu^+ preferentially binds to specific residues, from which it does not dissociate during the experiment. Peptides that do not possess basic amino acids do not strongly bind Cu^+, and $[M+Cu]^+$ ions for these peptides are not observed by MALDI. We observe that Cu^+ prefers to bind to arginine, lysine, and histidine because only fragment ions containing Cu^+ and basic amino acids are observed. Our results are in agreement with those published by Wesdemiotis on the relative ordering of copper binding affinity for the 20 common amino acids as determined by the kinetic method [19] and their more recent data for metal ion interactions with bradykinin and the des-arginine derivatives of bradykinin [20]. This article reports results from electronic structure calculations on the energetics of Cu^+ binding to model compounds and illustrates how Cu^+ binding energies influence fragmentation reactions of $[M+Cu]^+$ peptide ions.

2. Experimental approach

All metastable ion (MI) spectra were acquired using a Perseptive Biosystems Voyager Elite XL in delayed extraction-reflectron time-of-flight (DE-RTOF) mode, using a nitrogen laser (337 nm) for desorption/ionization [21,22]. Peptides obtained from Sigma (St. Louis, MO): his-leu-gly-leu-ala-arg (HLGLAR), Angiotensin II (DRVYIHPF), Angiotensin III (RVYIHPF), lys-bradykinin (KPPGFSPFR), and B-chain insulin fragment (RGFFYTPKA) were used without further purification as was the matrix, α-cyano-4-hydroxycinnamic acid obtained from Aldrich (Milwaukee, WI). Matrix and analyte were mixed with a matrix:analyte molar ratio of 1500:1 and co-deposited onto the copper sample stage (fabricated in house) using a dried-droplet method. In each case, a total of 5 pmol of analyte was deposited.

3. Computational approach

Electronic structure calculations were performed on both model systems and single amino acids to access monodentate and bidentate interactions respectively. All calculations are performed on one of several Silicon Graphics (R10000 processor) computers using the GAUSSIAN 94 suite of programs [5].

Monodentate structures were optimized as positively charged singlets using second-order Møller-Plesset (MP2) perturbation theory [23–25]. Frequency calculations were performed to determine if the optimized geometry was a minimum on the potential energy surface. Basis set superposition errors (BSSE) were also calculated using the counterpoise approximation [26,27] to correct the binding energy for basis

set effects. Geometry optimizations were carried out using Dunning's [28] triple-ζ plus polarization (TZP) basis set (C *d*: ζ=0.72; N *d*: ζ=0.8; O *d*: ζ=1.28; S *d*: ζ=0.542; H *d*: ζ=1.0) for all nonmetal atoms. The basis set used for copper was of triple-ζ quality in *s* and *p* space and of quadruple-ζ quality in *d* space [7511/7411/3111] and employs an effective core potential developed by Ermler and co-workers [29]. Optimized 4*s* and 4*p* orbitals [30,31] are included in the metal basis set, since it has been shown that these orbitals are particularly important in systems where most of the metal–ligand interaction occurs through these orbitals [σ donation to the $Cu^+)d^{10}$)].

Bidentate structures were generated using the CERIUS[2] (Molecular Simulations Inc., CA) suite of programs [32]. Amino acid plus Cu^+ ($AA+Cu^+$) isomers were then energy minimized using molecular mechanics methods that employed the Universal Force Field (UFF) of Goddard and co-workers [33]. Simulated annealing molecular dynamics calculations were performed on all structures (NVE, 1500K midcycle temperature, 12 ps at 0.001 ps/step) to remove strain from the ring system created by the Cu^+ bidentate interaction. The lowest energy conformer found was used as input for further geometry optimizations using ab initio and density functional methods.

Density functional theory [34], specifically the Becke-style three parameter using the Lee-Yang-Parr correlation functional (B3LYP) [35,36], has been shown to yield accurate geometries for first-row transition metal monocations, and is computationally more efficient than correlated ab initio methods [37,38]. B3LYP, which consists of Becke's hybrid three parameter exchange functional [36] and the Lee, Yang, Parr correlation functional [35], is employed for all geometry optimizations and frequency calculations at the density functional level in this study. First row atoms are treated with Dunning's double-ζ [39] basis set, with polarization functions added to oxygen and nitrogen (N: D=0.800, O: D=0.850) [basis set denoted as DZ(*p*)]. The basis set used for copper is identical to that used for mondentate calculations [30,31].

Various asparagine isomers were optimized at both B3LYP [35,36] and MP2 levels [23] of theory using the same basis sets to access the performance of B3LYP for this application, as previous studies indicate that MP2 produces reliable structures and binding energies for Cu^+ systems [40]. Structure comparison verifies that B3LYP provides accurate geometries for complexes of this size and composition. Energy calculations were also performed at the MP2 level on each structure without BSSE corrections, as results obtained by this methodology on monodentate systems were in agreement with experimental and other theoretical data [41].

4. Results

MI spectra were recorded for five peptides containing basic amino acids (arginine, histidine, lysine) in different positions (e.g. N-terminal, C-terminal, internal). These peptides were selected to probe the effect of basic amino acid position in the peptide sequence on Cu^+ binding sites and affinities. All fragment ions observed in Figs. 1–5 remain complexed to Cu^+ and are labeled using the nomenclature proposed by Roepstorff [42] for backbone cleavages. Fig. 1 shows the MI spectrum of HLGLAR $[M+Cu]^+$ ions where an immonium ion of arginine $\{[(a_6y_1)_1+Cu]^+\}$, N-terminal, and C-terminal fragment ions containing Cu^+ are observed, indicating competitive Cu^+ binding between the N-terminal histidine and C-terminal arginine. Angiotensin II (DRVYIHPF) $[M+Cu]^+$ ions (Fig. 2) dissociate into N-terminal fragment ions beginning at the second amino acid, arginine ($[a_2+Cu-H]^+$), C-terminal fragment ions following histidine ($[y_3+Cu+H]^+$), and internal fragment ions containing histidine. Competition for Cu^+ between arginine and histidine is again observed, as demonstrated by detection of fragment ions containing either histidine (18%–24%of the MI current) or arginine (76%–82% of MI current) [18,43]. Conversely, metastable dissociation of angiotensin III (RVYIHPF) $[M+Cu]^+$ ions (Fig. 3) yields predominately N-terminal fragment ions with a low abundance of internal and C-terminal fragment ions containing histidine (less than 8% of the MI current). Lysbradykinin (KPPGFSPFR) $[M+Cu]^+$ ions dissociate

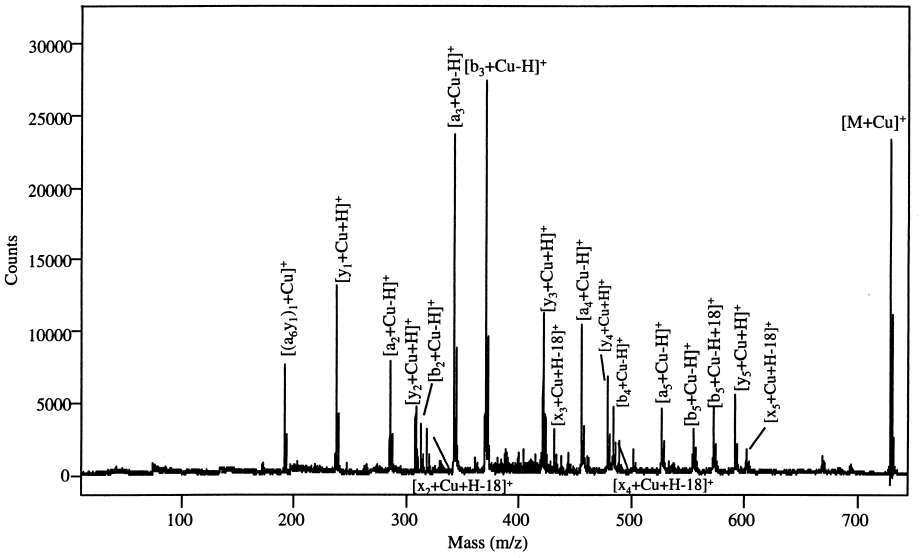

Fig. 1. Metastable ion spectrum of HLGLAR $[M+Cu]^+$ ions. $[(a_6y_1)_1+Cu]^+$ is an internal fragment ion that represents the arginine immonium ion. A number of N-terminal (a_n, b_n) fragment ions are observed, indicating that histidine possesses a relatively large Cu^+ binding affinity.

into N-terminal fragment ions containing lysine and Cu^+ (50%–55% of the MI current) and C-terminal fragment ions containing arginine and Cu^+ (40%–45% of the MI current). Fig. 5 displays the MI spectrum for the insulin B-chain fragment 22-30 (RGFFYTPKA) $[M+Cu]^+$ ions. Note, all fragment ions contain the N-terminal arginine, and the only fragment ion that contains lysine is the low abundance

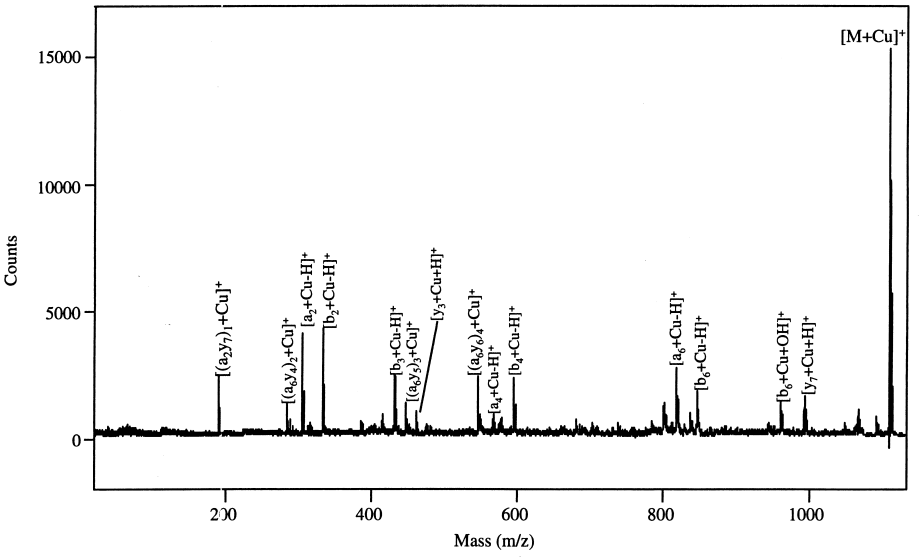

Fig. 2. Metastable ion spectrum of angiotensin II (DRVYIHPF) $[M+Cu]^+$ ions. Several internal fragment ions are present (e.g. $[(a_6y_6)_4+Cu]^+$) that contain histidine and not arginine, suggesting that histidine's affinity for Cu^+ is relatively large even when it is not N-terminal.

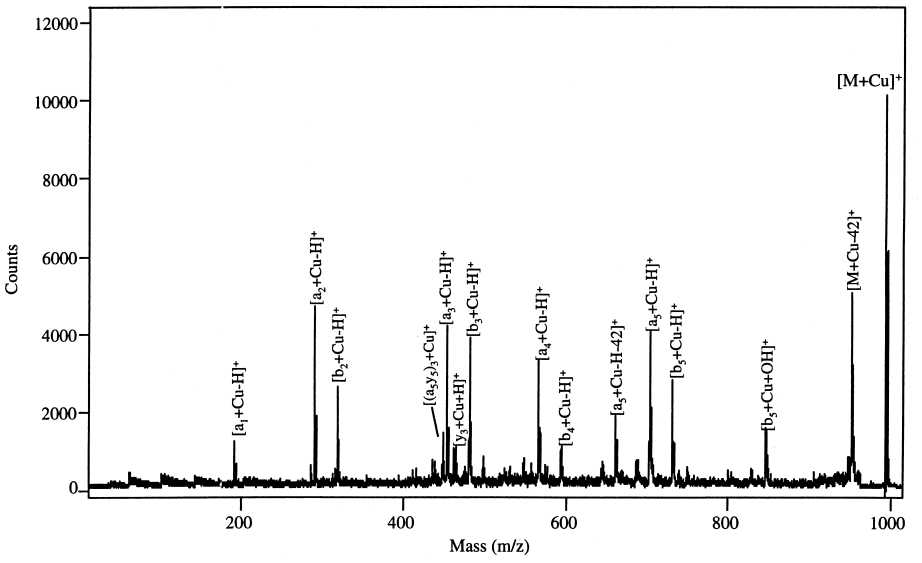

Fig. 3. Metastable ion spectrum of angiotensin III (RVYIHPF) $[M+Cu]^+$ ions. With the exception of one internal fragment ion, $[(a_5y_5)_3+Cu]^+$, all fragment ions are N-terminal (e.g. $[a_n+Cu-H]^+$), suggesting that arginine has a larger Cu^+ binding energy when it is N-terminal.

$[b_8+Cu-H]^+$ ion, indicating that Cu^+ binds strongly to the arginine with minimal interaction, if any, with lysine. Thus, initial inspection of the fragmentation patterns for $[M+Cu]^+$ peptide ions containing the pair of histidine and arginine or lysine and arginine suggests that the basic amino acids are Cu^+ ion binding sites but position in the amino acid sequence is critical to the Cu^+ binding affinities.

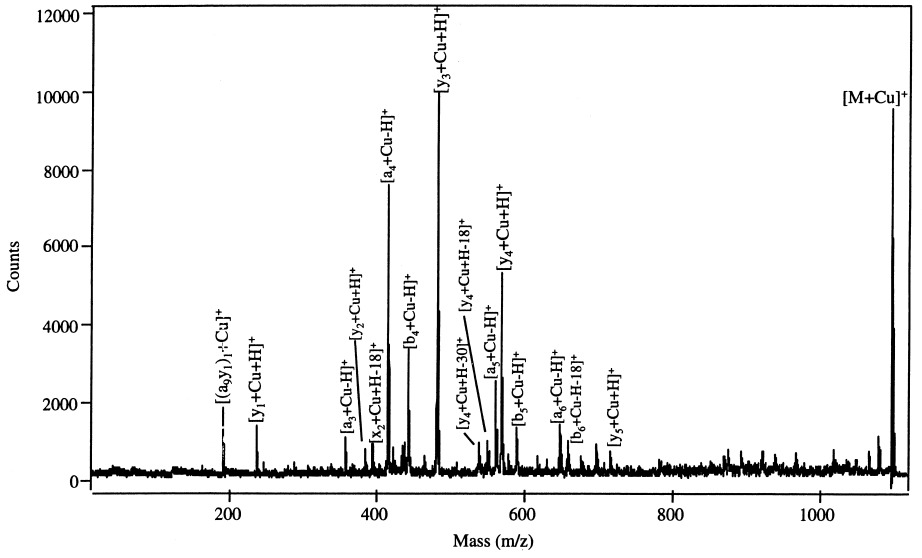

Fig. 4. Metastable ion spectrum of lys-bradykinin (LPPGFSPFR) $[M+Cu]^+$ ions. N-terminal (e.g. a_n and b_f) and C-terminal (e.g. y_n and x_n) ions are observed. Lysine fragment ions that do not contain arginine are present, implying that lysine possesses a relatively high Cu^+ affinity.

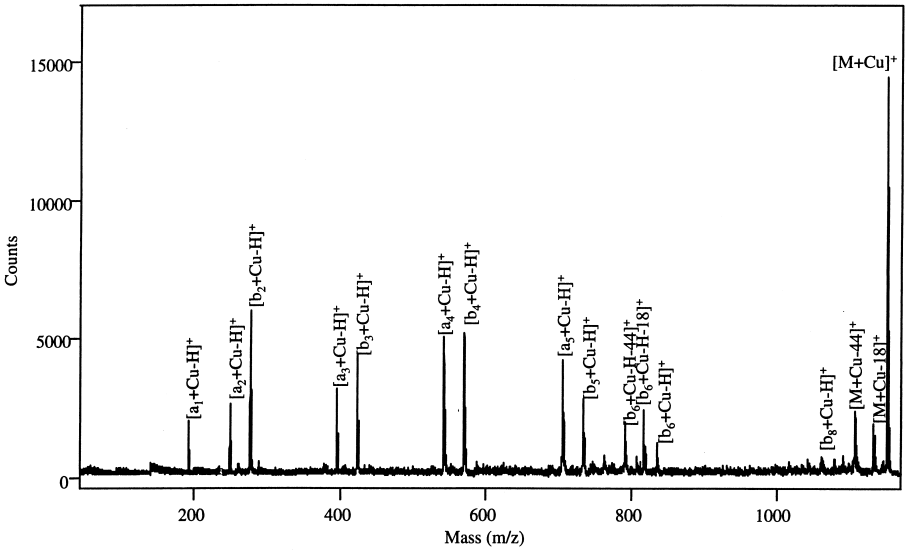

Fig. 5. Metastable ion spectrum of B-chain insulin fragment 22-30 (RGFFYTPKA) $[M+Cu]^+$ ions. No fragment ions are present that contain lysine and not arginine, suggesting that lysine is similar to arginine and has a different Cu^+ binding energy depending upon its position in the peptide.

4.1. Computations for Cu^+ complexation to model systems: monodentate

Cu^+ ion binding energies of several amino acids and/or their side chains are examined by theoretical methods of model systems that resemble amino acid functionalities. Monodentate ligand-Cu^+ model systems investigated are shown in Fig. 6, including several molecules for which comparative experimental and theoretical data are available [16,37,38,40,44,45]. Methanol [Fig. 6(A)], methanethiol [Fig. 6(B)], and methylamine [Fig. 6(C)] were chosen as models for serine, cysteine, and lysine side chains, respectively. The monodentate interaction of the side chain in Cu^+-histidine and Cu^+-arginine systems were modeled by Cu^+-imidazole [Fig. 6(D) and (E)] and Cu^+-methylguanidine [Fig. 6(F) and (G)] complexes. Ammonia [Fig. 6(H)], methylimine [Fig. 6(I)], hydrogen cyanide [Fig. 6(J)], acetonitrile [Fig. 6(K)], acetone [Fig. 6(L)], and pyridine [Fig. 6(M)] were also investigated to provide a comparison for our calculations with results obtained by alternate methods. Fig. 6 also shows the Cu^+ binding site in relation to the model system. In some cases more than one possible conformer was investigated to determine the preferential site for binding; however, only the lowest energy structure is reported.

Binding energies of Cu^+ with ammonia, methylimine, hydrogen cyanide, acetonitrile, acetone, and pyridine and their structures, shown in Fig. 6(D)–(I), are in good agreement with previously published work [16,46]. In these geometries, Cu^+ aligns with the lone electron pair on nitrogen or oxygen. It is interesting to note that the geometry for Cu^+-NH_3 compares best with that reported by Ohanessian and Hayou, in which they also used MP2 for optimization but employed an all electron basis sets on both the first row and transition metal atoms. Table 1 contains binding energies in which zero point energy, basis set superposition error and temperature contributions are included. These results compare favorably with theoretical and experimental results [16]. Previous work indicated that perturbation theory (MPn, n=2–4) overestimates relative energy differences [31] as well as binding energies [40]; however, due to the size of the molecular systems investigated here higher-level calculations are computationally too expensive. Because we are primarily interested in relative ordering

Table 1
Comparison of reported Cu^+ binding energies.

Model system	Uncorrected binding energy (kcal/mol)	ZPE corrected binding energy (kcal/mol)	ZPE and BSSE corrected binding energy (kcal/mol)	Experimental binding energies (kcal/mol)	Theoretical binding energies (kcal/mol)
Methanol	45.3	44.2	39.7	42[a]	42[c]
HCN	48.0	46.5	42.7		
Methane thiol	51.4	50.0	44.3	46[a]	48[c]
Acetone	49.7	48.7	44.4	48[a]	
Ammonia	59.2	56.5	50.6	57[b]	52.3[d],54.3[c], 54.7[f]
Acetonitrile	57.0	55.8	51.5	54[a]	
Methyl imine	60.1	58.1	53.1		55.1[d],56.4[c]
Methyl amine	62.3	60.0	54.2		59.0[d],58.1[c]
Pyridine	65.8	67.8	62.2	59[a]	
Imidazole	72.2	70.4	64.9	68[a]	
Methyl guanidine	80.1	79.1	72.8		78.7[e]

* Taken from [16]. Values reported were obtained by dividing the reported ΔH^0 values by 2. Experimental uncertainty is ±6 kcal/mol.
[b] Taken from [46]. Experimental uncertainty is ±3.6 kcal/mol.
[c] Taken from reference [40]. Reported values do not include a ZPE correction.
[d] Taken from reference [37]. Reported avlues include correction for the ZPE.
[e] Taken from reference [38]. Reported values do not include a ZPE correction.
[f] Taken from reference [48]. Reported values do not include a ZPE correction.

of Cu^+ binding affinities for the systems investigated, the more expedient, less expensive computational methods are appropriate.

In solution copper ions (Cu^+ and Cu^{2+}) are known to associate with amino acid side chains that contain sulfur, oxygen, and nitrogen. Geometry optimization yields staggered structures for methanethiol-Cu^+ (60° gauche) and methylamine-Cu^+ (180° gauche/anti) as shown in Fig. 6(B) and (C), whereas methanol-Cu^+ prefers an eclipsed structure as shown in Fig. 6(A). The difference in geometry for Cu^+ complexes with methanol and methanethiol is due to reduced *s* character of the sulfur orbitals. This type of structure is very different from those with alkali metal ions, which typically align with the dipole of a polar organic molecule [40]. Our structures compare well with those of Ohanessian, and calculated binding energies (Table 1) agree well with previous results from experiment and theory [16,37,40,45].

Observation of a cuprated histidine immonium ion from $[M+Cu]^+$ ions of HLGLAR indicates Cu^+ strongly binds to the side chain of histidine led us to calculate the binding energy of Cu^+ with imidazole. Two structures were investigated, one with Cu^+ bound at the secondary amine and the other with Cu^+ bound at the imino group. Results indicate that binding at the imino functionality is preferred, with an overall binding energy of 65 kcal/mol. Note that our calculated value agrees well with those reported by Deng and Kebarle [16] for 1-methyl-imidazole (~68 kcal/mol). The energetically preferred structure, in which Cu^+ binds to the imino group on imidazole, retains planarity, whereas no stable structure was found for Cu^+ binding at the secondary amine. Although we know of no theoretical literature involving this system, we feel that comparison with the work of Deng and Kebarle substantiates our relative binding energy.

Our results show that the arginine-Cu^+ binding energy is 73 kcal/mol, which is ~9 kcal/mol greater than that for any other amino acid. Although we were unable to locate experimental data for the Cu^+ binding energy to guanidine or methylguanidine, Luna and co-workers [38] investigated guanidine-Cu^+ binding by theoretical methods and found a similar binding energy as shown in Table 1. Both our results and those of Luna et al. suggest that Cu^+ preferentially binds to the imino group [Fig. 6(K)].

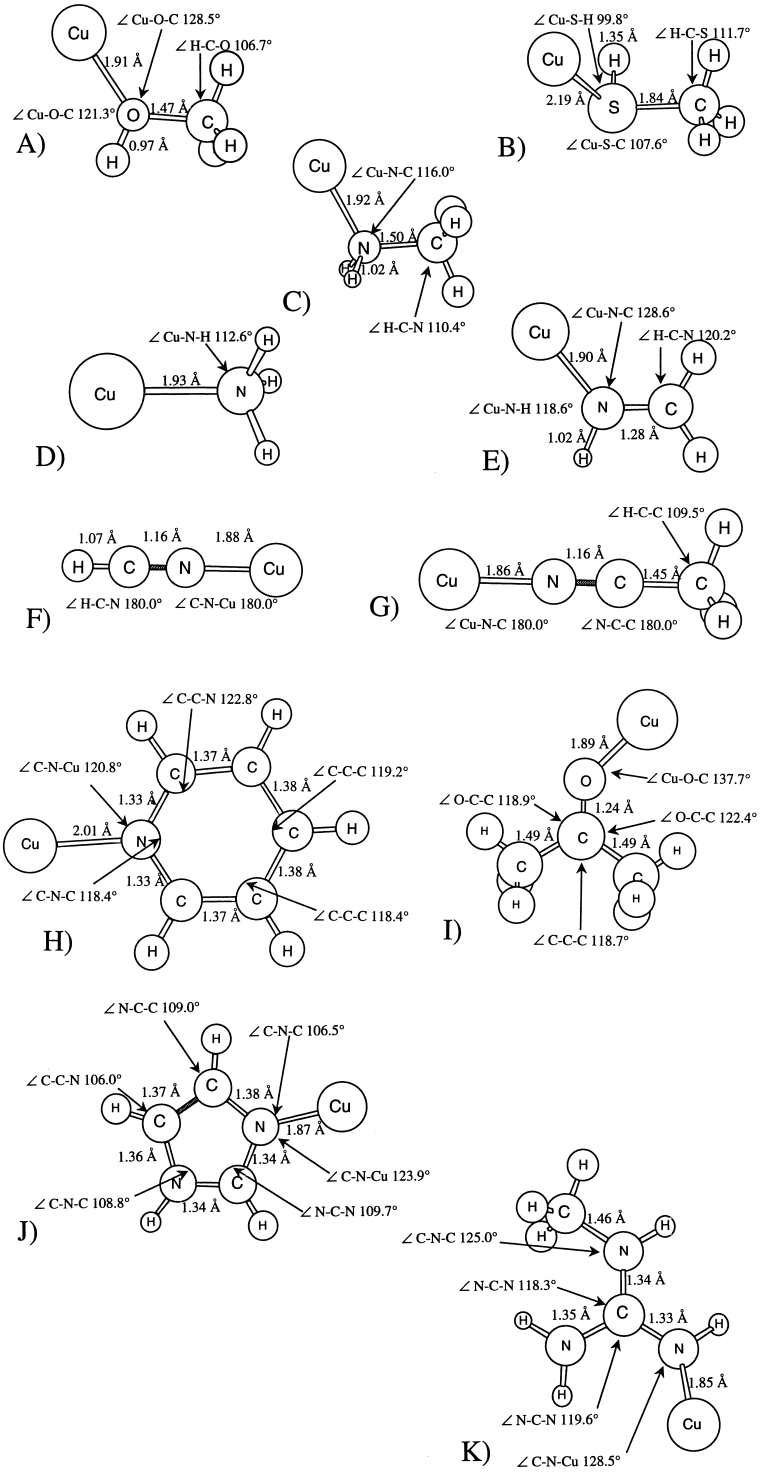

Fig. 6 Model systems investigated depicting Cu^+ orientation: (A) methanol, (B) methanethiol, (C) methylamine, (D, E) imidazole, (F, G) methylguanidine, (H) ammonia, (I) methylimine, (J) hydrogen cyanide, (K) acetonitrile, (L) acetone, (M) pyridine.

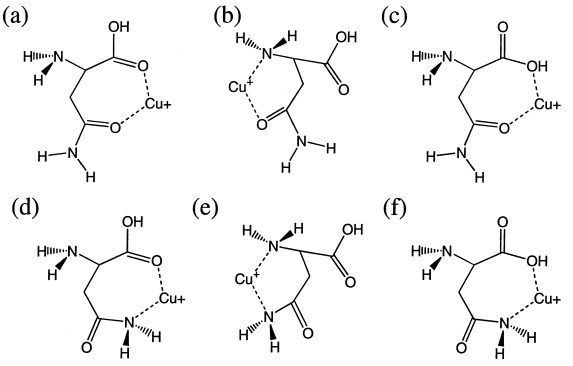

Fig. 7. Asparagine-Cu^+ isomers used to investigate different binding arrangements. (a) Asn_CO-Cu^+-CO, (b) Asn_CO-Cu^+-NH_2, (c) Asn_CO-Cu^+-OH, (d) Asn_NH_2-Cu^+-CO, (e) Asn_NH_2-Cu^+-NH_2, (f) Asn_NH_2-Cu^+-OH.

4.2. Computations for Cu^+ complexation to model systems: bidentate

The fragmentation chemistry of $[M+Cu]^+$ peptide ions suggests that the location of basic amino acids in the peptide sequence effects the Cu^+ binding affinity, calculations of bidentate amino acid-Cu^+ systems were undertaken. Numerous conformers and isomers are possible for the systems considered here; therefore, precautions to provide reasonable structures for energy calculations were taken. One such precaution was to examine various isomers made possible through Cu^+ binding at different functional groups. Due to the computational expense of high-level calculations on systems of this size, we examined asparagine as a model for various Cu^+ binding arrangements. Asparagine addresses the important forms of binding found in amino acid-Cu^+ complexes under consideration. Six isomeric structures of asparagine-Cu^+ were investigated (Fig. 7). Complexes are named by identifying the amino acid and the bonding ligands, specifying the side chain ligand first and the backbone ligand last (e.g. asp_NH_2-Cu^+-OH for *b* in Fig. 7). All isomers form stable six- or seven-membered rings and have Cu^+ binding energies that range from ~60 to 88 kcal/mol (Table 2).

Asparagine isomer geometries optimized at the B3LYP/DZ(*p*) were compared with MP2/DZ(*p*) geometries to ascertain whether B3LYP/DZ(*p*) generates accurate bond lengths and angles. Relevant geometrical parameters are included for both methods in Fig. 8 (MP2 in bold). Excellent agreement between the two methods is observed; therefore, B3LYP/DZ(*p*) was employed for all subsequent geometry optimizations and frequency calculations due to its computational efficiency. Energy calculations were performed on each geometry at the MP2 (MP2/TZP, [7511/7411/3111]) level (Table 2) for comparison with B3LYP binding energies.

Table 2
All energies are calculated at the B3LYP geometry (DZ on C and H; DZP on N and O; [7511/7411/3111] on Cu). Some difference is observed between the MP2 and B3LYP ordering, however the source of this disagreement will be addressed elsewhere.

Complex	B3LYP/DZ(*p*) [7511/7411/3111] (kcal/mol)	MP2/TZP [7511/7411/3111] (kcal/mol)
Arg_NH–Cu^+–NH_2	136.1	129.4
Lys_NH_2–CU^+–NH_2	120.4	115.8
His_N:−Cu^+–NH_2	110.0	101.8
Arg_NH_2–Cu^+–NH_2	106.8	101.27
Gln_CO–Cu^+–NH_2	102.6	91.7
Asn_CO–Cu^+–NH_2	98.5	87.8
Gln_CO–Cu^+–CO	97.4	84.8
Gln_NH_2–Cu^+–NH_2 94.15	88.9	
Asn_CO–Cu^+–CO	90.2	77.7
Asn_NH_2–Cu^+–NH_2	89.6	81.9
Glu_CO–Cu^+–CO	87.4	74.3
Asp_CO–Cu^+–CO	84.3	68.9
Asn_CO–Cu^+–OH	78.4	68.5
Asn_NH_2–Cu^+–CO	78.0	68.5
Asn_NH_2–Cu^+–OH	67.0	59.3

Optimized structures for Cu^+-amino acid complexes other than asparagine calculated at the B3LYP level are shown in Fig. 9. Stable six-, seven-, eight-, and nine-membered ring systems were found for the amino acid-Cu^+ systems investigated. Based on binding energies for the asparagine isomers, binding between side chain functional groups and the hydroxyl portion of the carboxylic acid were not investigated.

Two separate arginine-Cu^+ isomers were studied [Fig. 9(I) and (II)]. Both structures formed nine-membered rings that involved binding at the backbone NH_2 group but differed in the side chain functional

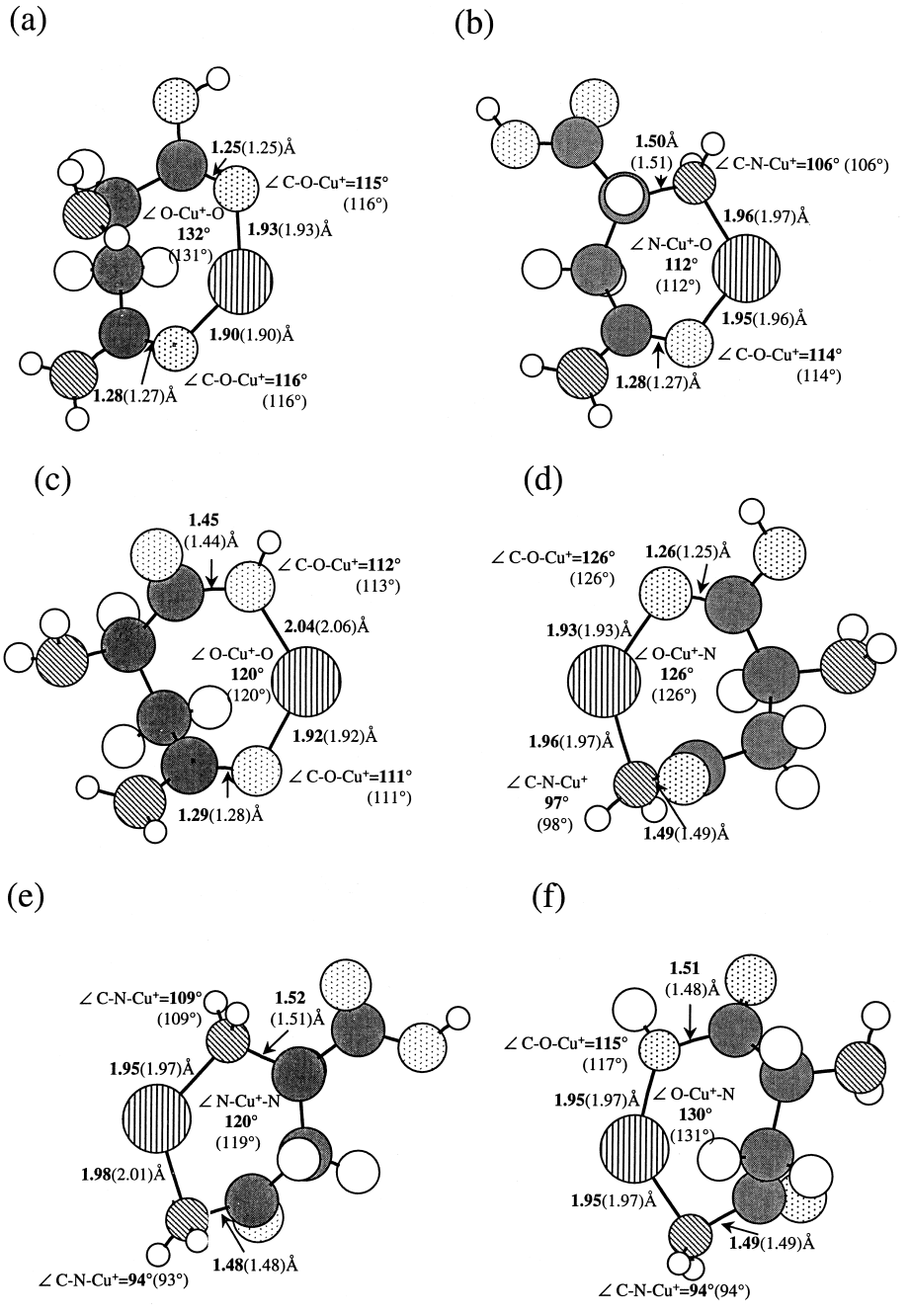

Fig. 8. Geometry optimized asparagine-Cu^+ isomers. MP2 results are in boldface type and B3LYP results are in plain type. (a) Asn_CO-Cu^+-CO, (b) Asn_CO-Cu^+-NH_2, (c) Asn_CO-Cu^+-OH, (d) Asn_NH_2-Cu^+-CO, (e) Asn_NH_2-Cu^+-NH_2, (f) Asn_NH_2-Cu^+-OH.

group that Cu^+ interacts with (NH_2 versus NH). Binding energies calculated for arg_NH-Cu^+-NH_2 and arg_NH_2-Cu^+-NH_2 at the B3LYP/DZ(*p*) level are 132.06 and 103.06 kcal/mol, respectively (Table 2). This agrees with previously calculated Cu^+ binding energies that found the guanidine imino group to have

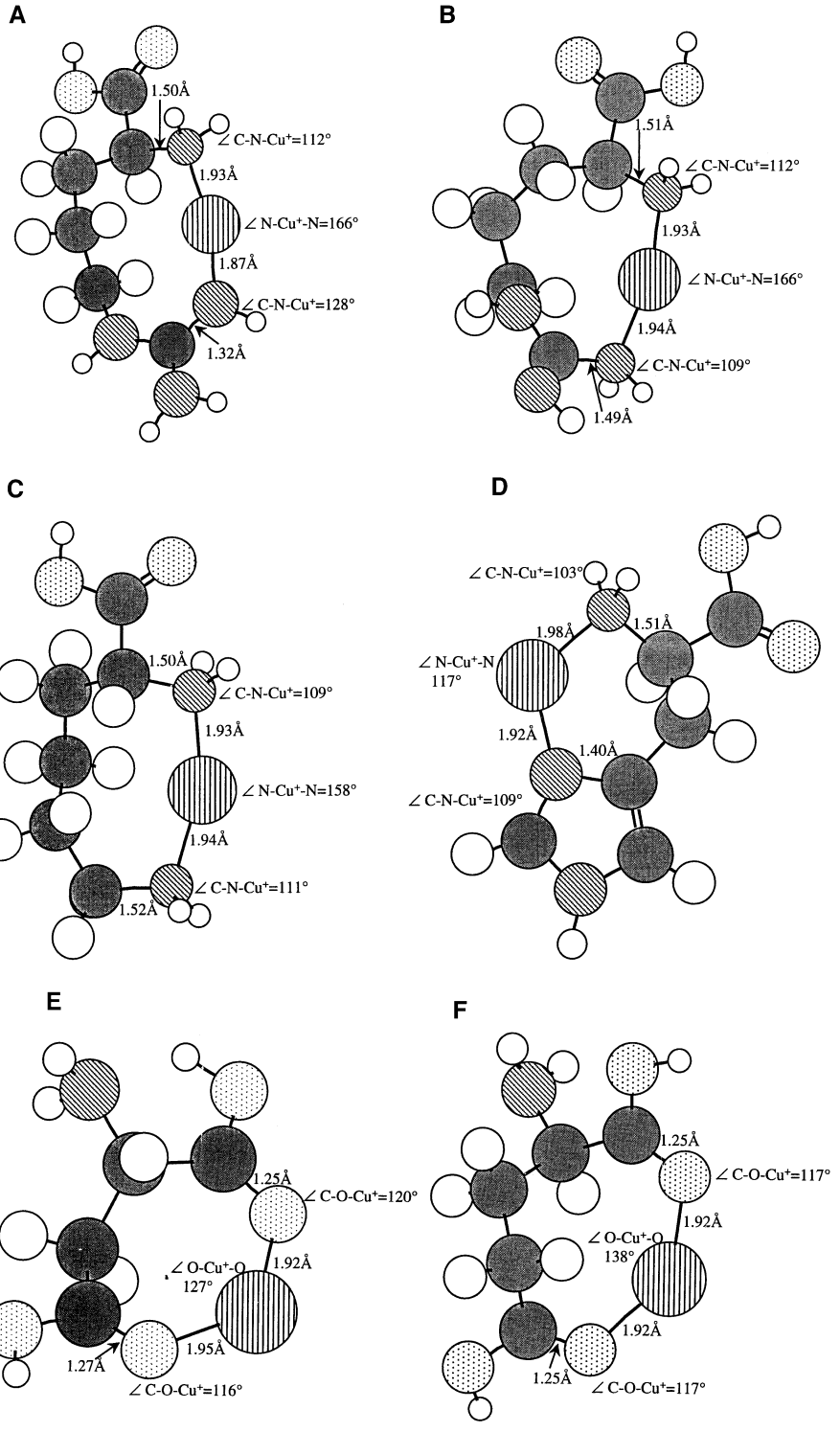

Fig. 9. Geometry optimized structures for amino acid-Cu^+ complexes obtained at B3LYP/DZ(p), [7511/7411/3111]. (I) arg_NH-Cu^+-NH_2, (II) arg_NH_2-Cu^+-NH_2, (III) lys_NH_2-Cu^+-NH_2, (IV) his_N:-Cu^+-NH_2, (V) Asp_CO-Cu^+-CO, (VI) Glu_CO-Cu^+-CO, (VII) Gln_CO-Cu^+-CO, (VIII) Gln_NH_2-Cu^+-NH_2, (IX) Gln_CO-Cu^+-NH_2.

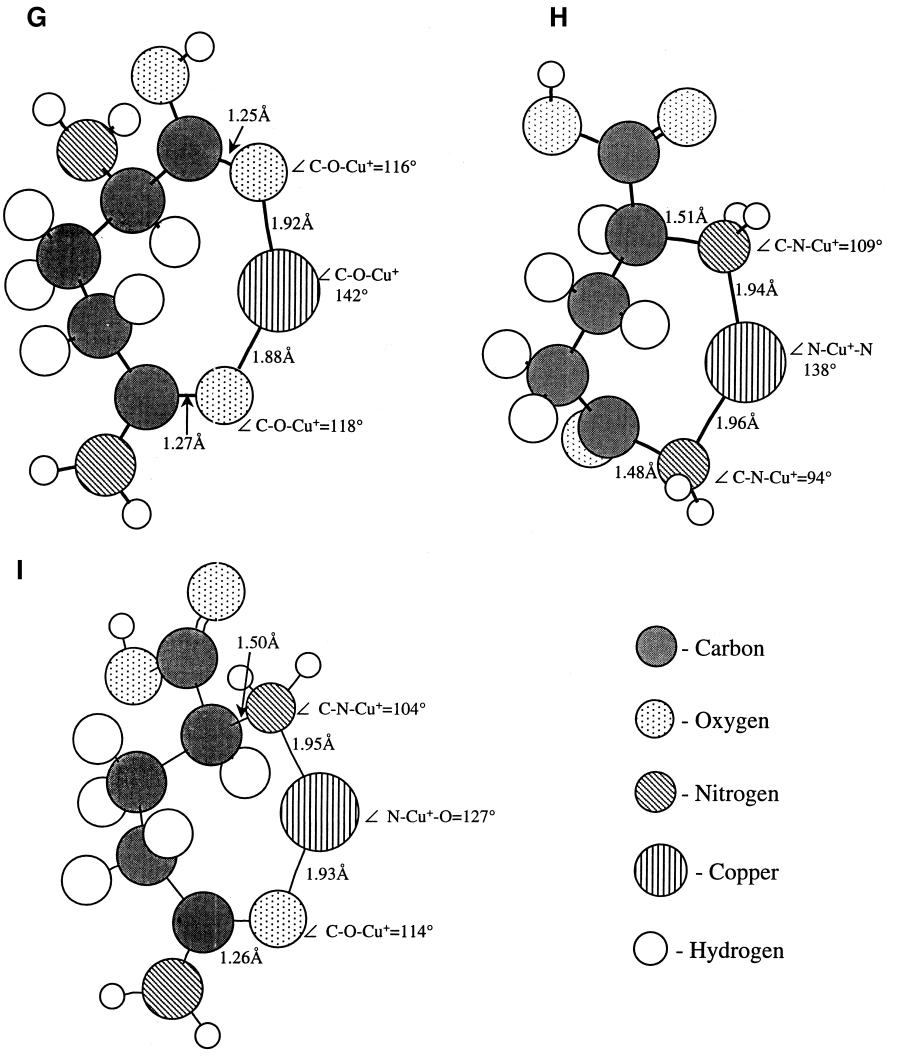

Fig. 9. (*continued*)

the highest Cu^+ binding affinity of the model systems studied.

Binding energies for bidentate lysine-Cu^+ and histidine-Cu^+ complexes calculated at the B3LYP/DZ(*p*) level are 116.31 and 107.70 kcal/mol, respectively. Cu^+ preferentially binds to lysine between the side chain and backbone NH_2 groups [Fig. 9(III)] forming an eight-membered ring. Cu^+ forms a very stable six-membered ring with the backbone NH_2 group and the imidazole imino group of histidine [Fig. 9(IV)]. No other isomers for either of these amino acids were investigated based on prior results on model systems that indicated that other interactions would be less favorable.

Experimental work on alkali metals complexed to polymers (synthetic and biological) suggested that the alkali metal ion was complexed to several carbonyl groups. Prior theoretical and experimental results suggest that Cu^+ binds to nitrogen more strongly than oxygen [16,40]. To verify that this holds true for bidentate Cu^+ interactions we examined both aspartic-Cu^+ and glutamic-Cu^+ complexes. In each com-

plex, Cu^+ interacts with the carboxylic acid carbonyl groups [Fig. 9(V) and (VI)] forming a seven-membered ring with aspartic acid and an eight-membered ring with glutamic acid. The Cu^+ binding energies for aspartic and glutamic acid are 82.93 and 86.09 kcal/mol, respectively [at the B3LYP/DZ(*p*) level].

Glutamine-Cu^+ was also studied to determine if it would bind Cu^+ more tightly than the basic amino acids studied. Three isomers were investigated based on results for asparagine: Gln_NH_2-Cu^+-NH_2, Gln_CO-Cu^+-NH_2 and Gln_CO-Cu^+-CO. Like asparagine, Gln_CO-Cu^+-NH_2 has the largest Cu^+ binding energy of 102 kcal/mol whereas Gln_CO-Cu^+-CO and Gln_NH_2-Cu^+-NH_2 have binding energies of 95.61 and 91.24 kcal/mol, respectively.

5. Discussion

The fragmentation reaction chemistry of $[M+H]^+$ peptide ions is adequately described in terms of a "mobile proton model"[7]. That is, if a peptide contains multiple basic sites, e.g. N-terminus, backbone amide groups, and basic amino acid side chains (arginine, lysine, histidine, asparagines, and glutamine), the energy required to move the H^+ from one basic site to another is rather small resulting in charge-directed fragmentation. Conversely, studies on metal ion-peptide complexes indicate that metal ions are coordinated at specific sites of the molecule and there are substantial energy/kinetic barriers to moving the metal ions from one site to another, leading to more specific fragmentation reactions, and less complex mass spectra [8,15,47]. In earlier articles, we suggested that the number of Cu^+ adducts to peptides has a direct correlation to the number of basic amino acids [6], and fragmentation of peptide-Cu^+ complexes is controlled by the absence or presence of basic residues that bind Cu^+ strongly [43]. Experimental and theoretical data indicate that Cu^+ is anchored (i.e. no migration or dissociation) at N-terminal basic residues in peptides via a bidentate binding arrangement at a minimum. $[M+Cu]^+$ peptide ion fragmentation chemistry is dictated by the anchored Cu^+ ion and interactions which it may have with other basic residues or backbone functional groups (e.g. C&z.dnd;O, NH); however, to fully understand such interactions and their affect on fragmentation chemistry, a detailed and systematic study must be performed. In the following paragraphs, correlation between theoretically calculated binding energies and experimental data for interpreting fragment ion spectra of peptide-Cu^+ complexes is provided.

We obtain binding energies for model monodentate-Cu^+ ligand systems that agree to within ~3 kcal/mol of previously published data [16,37,38,40,48]. Values obtained in this study are systematically low when compared with previously reported numbers owing to the different method used [MP2 versus coupled cluster single double (triple)], but the relative binding energies do not differ. For example, relative binding energies of the model monodentate ligand-Cu^+ systems extrapolated to amino acid-Cu^+ complexes are as follows:

arginine > histidine > lysine > cysteine > serine

Calculated bidentate Cu^+ binding energies for individual amino acids yield a slightly different relative copper affinity shown below, indicating the importance of multidentate Cu^+ coordination:

Arg > Lys > His > Gln > Asn > Glu > Asp

The peptides HLGLAR, angiotensin II (DRVYIHPF), angiotensin III (RVYIHPF), lys-bradykinin (KPPGFSPFR), and B-chain insulin fragment (RGFFYTPKA) each contain two basic amino acids where their position is varied (e.g. N-terminal, C-terminal, and internal). A comparison of the observed N-terminal, C-terminal, and internal fragment ions and their abundances provides information on the Cu^+ ion binding site and relative binding energy. For example, each of the five $[M+Cu]^+$ ions yields abundant fragment ions that contain arginine and Cu^+ regardless of arginine's position in the amino acid sequence at the N-terminus, C-terminus, or internal. In addition, common to each MI spectrum is the cuprated arginine immonium ion (*m/z* 191), where H^+ is replaced by Cu^+ (R-CH-$NHCu^+$ where R is the side chain). This suggest that

arginine is a primary Cu^+ binding site with a large binding affinity. Our calculations of the monodentate ligand-Cu^+ systems support this assumption as the monodentate model for arginine, methyl guanidine, has the greatest Cu^+ ion affinity by 8 kcal/mol, whereas the arginine-Cu^+ bidentate binding arrangement is ~15 kcal/mol stronger than other bidentate binding arrangements. In Figs. 2 and 3, C-terminal fragment ions are first observed at histidine, $[y_3+Cu+H]^+$, and internal fragment ions are observed containing histidine and not arginine, $[(a_6y_n)_{n-2}+Cu]^+$ where $n=4, 5, 6$. This demonstrates that histidine is a primary Cu^+ binding site, which is also supported by theory with the imine nitrogen of imidazole having a monodentate Cu^+ binding energy of ~65 kcal/mol and a bidentate Cu^+ binding energy of ~110 kcal/mol. The abundant N-terminal fragment ions in lys-bradykinin (KPPGFSPFR) (Fig. 4) also suggest that lysine readily binds Cu^+. These data imply that histidine and lysine may be interacting with Cu^+ instead of or simultaneously with arginine. Therefore, Cu^+ retention is dependent upon relative binding energies (e.g. competitive processes), or the fragmentation chemistry is sampling different gas-phase structures with Cu^+ anchored at the different amino acids.

The MI spectrum of HLGLAR $[M+Cu]^+$ ions (Fig. 1) contains abundant N-terminal fragment ions despite the presence of a C-terminal arginine. For example, 65%–70% of the metastable ion current is due to histidine containing fragment ions, whereas only 25%–30% of the fragment ions contain arginine. This trend in fragment ion abundances contradicts the both monodentate and bidentate ligand-Cu^+ calculations that predict arginine to have 8 and 26 kcal/mol, respectively, greater Cu^+ binding energy than histidine. Based on calculations of monodentate and bidentate systems, we would expect the fragment ion spectra to be dominated by C-terminal fragment ions containing arginine and Cu^+. On the other hand, the MI spectra of angiotensin II (DRVYIHPF) and angiotensin III (RVYIHPF) contain histidine as an internal amino acid and less than 18%–24% and 3%–8% of the MI current, respectively, consists of fragment ions containing histidine without arginine. Comparison of the fragmentation chemistry for these three $[M+Cu]^+$ peptide ions not only indicates that histidine binds Cu^+, but suggests that residue location plays a role in stabilizing the Cu^+-peptide interaction and increases the Cu^+ affinity of the N-terminal histidine in HLGLAR. Electronic structure calculations on histidine-Cu^+ complexes indicate that a stable six-membered ring is formed when Cu^+ interacts with the N-terminus and the imidazole imine functionality. The bidentate interaction is ~30 kcal/mol stronger than monodentate binding of Cu^+ to the imidazole imine group only, indicating that multidentate binding is occurring and must be accounted for in spectral interpretation.

Abundant lysine containing fragment ions (50%–55% of the MI current) are observed in the MI spectra of lys-bradykinin (KPPGFSPFR) $[M+Cu]^+$ ions (Fig. 4). Given the calculated binding energies for lysine and arginine monodentate model systems differ by ~18 kcal/mol, we expected the abundance of arginine containing fragment ions to be greater than that for lysine containing ions. To probe whether

N-terminus would explain the apparent increase in arginine Cu^+ binding affinity for angiotensin III, which has an N-terminal arginine, relative to angiotensin II in which arginine is an internal amino acid. Calculated Cu^+ binding energies for bidentate arginine-Cu^+ complexes confirm that two stable isomers are possible as shown in Fig. 9(I) and (II). The energetically preferred isomer [Fig. 9(I)], in which the guanido imine functionality and the N-terminal amine group complex Cu^+, is more stable than calculated lysine-Cu^+ and histidine-Cu^+ bidentate structures investigated by ~15 and ~28 kcal/mol, respectively. These data along with results from Cerda and Wesdemiotis [19] confirm that arginine with an unblocked N-terminal amine group has the highest Cu^+ affinity, which will determine observed fragment ions in peptides and proteins (containing arginine) complexed to Cu^+.

Experimental and theoretical results are in good agreement, indicating that Cu^+ preferentially binds to an N-terminal arginine, if present, and is not displaced during the dissociation process. Evidence of strong bidentate Cu^+ binding to histidine, lysine, and arginine is observed in theory and supported by experimental results. Neither fragmentation reactions nor calculated binding energies suggest that Cu^+ favors binding to oxygen bases, as is suggested for alkali metal ions. Copper binding differs from that for alkali metal cations due to hard and soft acid base principles as suggested by Deng and Kebarle [16] and discussed in detail by Shields et al. [43]. Although direct binding of Cu^+ to oxygen bases is not energetically favorable relative to nitrogen bases, stabilization of Cu^+ by means of interactions by oxygen bases on the backbone or side-chain functional groups which mimic "solvation" is not ruled out. Cu^+ solvation by oxygen bases requires that the molecule adapt a conformation that places oxygen atoms in close proximity with the N-terminus, since Cu^+ will be bound there in cases where the N-terminus is a basic residue. In molecules with or without a basic residue at the N-terminus Cu^+, solvation is determined by entropic and steric effects; however discussion of this topic is beyond the scope of this article.

6. Conclusion

Through a combination of electronic structure calculations and experimental data, we have determined that copper preferentially binds to basic residues and establishes a relative copper affinity scale for the modeled systems based on monodentate and bidentate interactions. It must be noted that bidentate or multidentate binding of Cu^+ by basic side chains must be considered for correct interpretation of MI spectra. The calculated relative ordering of Cu^+-amino acid residues correlates well with our experimental observations and those of Cerda and Wesdemiotis [19]. However, there is some disparity between the calculated ordering of asparagine and glutamic acid with that of Cerda and Wesdemiotis which may be due to consideration of a local rather than a global minimum or entropic effects (i.e. reverse activation barrier) that are not handled well by the kinetic method. For peptides with more than one residue, Cu^+ binding between multiple basic residues (e.g. arginine and lysine, arginine and histidine, or lysine and histidine) must also be addressed since strong Cu^+ binding bidentate structures increase the overall peptide-Cu^+ binding energy. The strong binding of Cu^+ opens the possibility of transition metal ions being used to complex at selective sites in peptides and proteins, thus changing the local and possibly global conformation of the molecular system. Ion mobility measurements on specifically chosen peptides would help to determine how Cu^+ is interacting with basic residues (e.g. competitive binding) and how a peptide's conformation changes with varying location of arginine (e.g. solvation by oxygen bases).

Acknowledgements

The authors acknowledge the National Science Foundation (NSF) under grant nos. CHE-9629966 and CHE-9528196 and the Robert A. Welch Foundation for funding this research. They would also like to thank the Texas A&M University Supercomputer facility for allotting computer time on the 24-processor and 32-processor SGI supercomputers. One of the authors (B.K.B.) would like to thank Dr. Lisa Thom-

son and Dr. Agnes Derecskei-Kovacs for helpful discussions regarding the calculations.

References

[1] A.E. Martell, Metal Complexes in Aqueous Solutions, Plenum, New York, 1996.
[2] D.H. Russell, Gas Phase Inorganic Chemistry, D.H. Russell (Ed.), Plenum, New York, 1989, p. 412.
[3] B.S. Freiser, Organometallic Ion Chemistry, B.S. Freiser (Ed.), Kluwer Academic, Boston, 1996, Vol. 15, p. 335.
[4] M.F. Guest, J.H.V. Lenthe, J. Kendrick, K. Schoffel, P. Sherwood, R.D. Amos, R.J. Buenker, M. Dupuis, N.C. Handy, I.H. Hillier, P.J. Knowles, V. Bonacic-Koutecky, W.v. Niessen, R.J. Harrison, A.P. Rendell, V.R. Saunders, A.J. Stone, GAMESS-UK, Computing for Science, Ltd., Daresbury Laboratory, 1995.
[5] M.J. Frisch, G.W. Trucks, H.B. Schlegel, P.M.W. Gill, B.G. Johnson, M.A. Robb, J.R. Cheeseman, T.A. Keith, G.A. Petersson, J.A. Montgomery, K. Raghavachari, M.A. Al-Laham, V.G. Zakrzewski, J.V. Ortiz, J.B. Foresman, C.Y. Peng, P.A. Ayala, M.W. Wong, J.L. Andres, E.S. Replogle, R. Gomperts, R.L. Martin, D.J. Fox, J.S. Binkley, D.J. Defrees, J. Baker, J.P. Stewart, M. Head-Gordon, C. Gonzalez, J.A. Pople, Gaussian 94, 3rd ed., Gaussian, Inc., Pittsburgh, PA, 1995.
[6] S.J. Shields, B.K. Bluhm, D.H. Russell, Int. J. Mass Spectrom. Ion Processes 182/183 (1999) 185.
[7] A.R. Dongre, J.L. Jones, A. Somogyi, V.H. Wysocki, J. Am. Chem. Soc. 118 (1996) 8365.
[8] O.V. Nemirovskiy, M.L. Gross, J. Am. Soc. Mass Spectrom. 7 (1996) 977.
[9] D.H. Russell, E.S. McGlohon, L.M. Mallis, Anal. Chem. 60 (1988) 1818.
[10] M.L. Gross, Int. J. Mass Spectrom. Ion Processes 118 (1992) 137.
[11] L.M. Teesch, J. Adams, J. Am. Chem. Soc. 113 (1991) 812.
[12] T. Wyttenbach, G. von Helden, M.T. Bowers, J. Am. Chem. Soc. 118 (1996) 8355.
[13] L.M. Mallis, D.H. Russell, Int. J. Mass Spectrom. Ion Processes 78 (1987) 147.
[14] C.Q. Jiao, B.S. Freiser, S.R. Carr, C.J. Cassady, J. Am. Soc. Mass Spectrom. 6 (1995) 521.
[15] O.V. Nemirovsky, M.L. Gross, J. Am. Soc. Mass Spectrom. 7 (1997) 977.
[16] H. Deng, P. Kebarle, J. Am. Chem. Soc. 120 (1998) 2925.
[17] S. Mahapatra, J.A. Halfen, E.C. Wilkinson, G. Pan, X. Wang Jr., C.J. Cramer Jr., W.B. Tolman, J. Am. Chem. Soc. 118 (1996) 11555.
[18] S.J. Shields, B.K. Bluhm, D.H. Russell, J. Am. Soc. Mass Spectrom. 11 (2000) 626.
[19] B.A. Cerda, C. Wesdemiotis, J. Am. Chem. Soc. 117 (1995) 9734.
[20] B.A. Cerda, L. Cornett, C. Wesdemiotis, Int. J. Mass Spectrom. 193 (1999) 205.
[21] M.L. Vestal, P. Juhasz, S.A. Martin, Rapid Comm. Mass Spectrom. 9 (1995) 1044.
[22] R.D. Edmondson, D.H. Russell, J. Mass Spectrom. 32 (1997) 263.
[23] C. Møller, M.S. Plesset, Phys. Rev. 46 (1936) 618.
[24] J.D. Watts, M. Dupuis, J. Comput. Chem. 9 (1988) 158.
[25] J.E. Rice, R.D. Amos, N.C. Handy, T.J. Lee, H.F. Schaefer, J. Chem. Phys. 85 (1986) 963.
[26] S.F. Boys, F. Bernardi, Mol. Phys. 19 (1970) 553.
[27] K.R. Liedl, J. Chem. Phys. 108 (1998) 3199.
[28] T.H. Dunning, J. Chem. Phys. 55 (1971) 716.
[29] M.M. Hurley, L. Fernandez-Pacios, P.A. Christiansen, R.B. Ross, W.C. Ermler, J. Chem. Phys. 84 (1986) 6840.
[30] M. Couty, M.B. Hall, J. Comput. Chem. 17 (1996) 1359.
[31] M. Couty, C.A. Bayse, R. Jimenez-Catano, M.B. Hall, J. Phys. Chem. 100 (1996) 13976.
[32] M.S. Inc., J. Mol. Graph. Model. 15 (1997) 63.
[33] A.K. Rappe, C.J. Casewit, K.S. Colwell, W.A. Goddard, W.M. Skiff, J. Am. Chem. Soc. 114 (1992) 10024.
[34] W. Kohn, L.J. Sham, Phys. Rev. A 140 (1965) A1133.
[35] C. Lee, W. Yang, R.G. Parr, Phys. Rev. B 92 (1988) 785.
[36] A.D. Becke, J. Chem. Phys. 98 (1993) 5648.
[37] A. Luna, B. Amekraz, J. Tortajada, Chem. Phys. Lett. 266 (1997) 31.
[38] A. Luna, B. Amekraz, J.-P. Morizur, J. Tortajada, O. Mo, M. Yanez, J. Phys. Chem. 101 (1997) 5931.
[39] T.H. Dunning, P.J. Hay, Methods of Electronic Structure Theory, T.H. Dunning, P.J. Hay (Eds.), Plenum, New York, 1977, Vol. 3.
[40] S. Hayou, G. Ohanessian, Chem. Phys. Lett. 280 (1997) 266.
[41] B.K. Bluhm, S.J. Shields, C.A. Bayse, M.B. Hall, D.H. Russell, Proceedings of the 46th Conference on Mass Spectrometry and Allied Topics, 1998, Orlando, FL.
[42] P. Roepstorff, Biomed. Mass Spectrom. 11 (1984) 601.
[43] S.J. Shields, B.K. Bluhm, D.H. Russell, unpublished.
[44] S. Hayou, G. Ohanessian, J. Am. Chem. Soc. 119 (1997) 2016.
[45] R.W. Jones, R.H. Staley, J. Am. Chem. Soc. 104 (1982) 2296.
[46] D. Walter, P.B. Armentrout, J. Am. Chem. Soc. 120 (1998) 3176.
[47] A.T. Blades, J.S. Klassen, P. Kebarle, J. Am. Chem. Soc. 118 (1996) 12437.
[48] S.R. Langhoff, C.W. Bauschlicher, H. Partridge, M. Sodupe, J. Phys. Chem. 95 (1991) 10677.